Earth and Planetary Science Letters 270 (2008) 189–199

Contents lists available at ScienceDirect

Earth and Planetary Science Letters

journal homepage: www.elsevier.com/locate/epsl

Sulfuric acid as an agent of carbonate weathering constrained by $\delta^{13}C_{DIC}$: Examples from Southwest China

Si-Liang Li [a], Damien Calmels [b,c], Guilin Han [a,*], Jérôme Gaillardet [b], Cong-Qiang Liu [a]

[a] The State Key Laboratory of Environmental Geochemistry, Institute of Geochemistry, Chinese Academy of Sciences, Guiyang 550002, China
[b] Equipe de Géochimie et Cosmochimie, Institut de Physique du Globe de Paris, Université Paris 7, 4 Place Jussieu, 75252 Paris Cedex 05, France
[c] Department of Earth Sciences, University of Cambridge, Downing Street, Cambridge, CB2 3EQ, UK

ARTICLE INFO

Article history:
Received 2 June 2007
Received in revised form 31 January 2008
Accepted 29 February 2008
Available online 18 March 2008

Editor: C.P. Jaupart

Keywords:
$\delta^{13}C$
carbonate weathering
sulfuric acid
Beipanjiang River
carbon cycle
anthropogenic activities

ABSTRACT

Rock weathering by carbonic acid is thought to play an important role in the global carbon cycle because it can geologically sequestrate atmospheric CO_2. Current model of carbon cycle evolution usually assumes that carbonic acid is the major weathering agent and that other acids are not important. Here, we use carbon isotopic evidence and water chemistry of springs and rivers from the Beipanjiang River basin (Guizhou Province, Southwest China) to demonstrate that sulfuric acid is also an important agent of rock weathering. The $\delta^{13}C$ of dissolved inorganic carbon (DIC) in the water samples ranges from −13.1‰ to −2.4‰, and correlates negatively to $[HCO_3^-]/([Ca^{2+}]+[Mg^{2+}])$ ratios and positively to $[SO_4^{2-}]/([Ca^{2+}]+[Mg^{2+}])$ ratios. These relationships are interpreted as mixing diagrams between two reactions of carbonate weathering, using carbonic acid and sulfuric acid as a proton donor, respectively. Mixing proportions show that around 42% of the divalent cations in the spring water from Guizhou are originated from the interaction between carbonate minerals and sulfuric acid. It is shown that 40% of this sulfuric acid is derived from the atmosphere and has an anthropogenic origin. The remaining 60% are derived from the oxidative weathering of sulfide minerals in sedimentary rocks. Our results show the positive action of sulfuric acid on the chemical weathering of carbonate. Particularly, we show that sulfuric acid generated by coal combustion has increased by almost 20% the weathering rates of carbonate in Southwest China. This is a clear evidence that human activities are changing the weathering rates of rocks and demonstrates a negative feedback on the acidification of the ocean by greenhouse gases. Because of the involvement of sulfuric acid in weathering reactions, 63% of the alkalinity exported by rivers is derived from carbonate, instead of 50% when atmospheric CO_2 is the only acid involved in chemical weathering of carbonate. In the Guizhou Province, the weathering of carbonate is thus, at least transiently, a net source of CO_2 to the atmosphere. When extrapolated at global scale, sulfuric acid-induced carbonate weathering could counterbalance a significant part of the CO_2 consumed by silicate weathering. This paper highlights the competition between silicate weathering by carbonic acid and carbonate weathering by sulfuric acid for the regulation of the atmospheric CO_2 level.

1. Introduction

Chemical weathering of rocks is one of the geological processes at the earth's surface that can remove CO_2 from the atmosphere converting it into DIC (dissolved inorganic carbon). This DIC is transported by rivers and thereafter precipitated in the ocean as carbonate minerals. Based on the inversion technique of geochemical data from large rivers, a flux of 0.15 PgC/yr is estimated for atmospheric CO_2 consumed by carbonate weathering reactions (Gaillardet et al., 1999). The conventional view of C cycle modeling over geological timescale (Berner and Kothavala, 2001; Wallmann, 2001) assumes that the flux of CO_2 consumed by carbonate dissolution on the continents is balanced by the flux of CO_2 released to the atmosphere from the oceans by carbonate precipitation, which can be expressed as follows:

$$CaCO_3 + CO_2 + H_2O \rightarrow Ca^{2+} + 2HCO_3^- \rightarrow CaCO_3 + CO_2 + H_2O \quad (1)$$

In those models, the production of alkalinity by the weathering of silicates is the only mechanism that is able to stabilize the atmospheric CO_2 content (Berner and Caldeira, 1997) because it leads to a net sequestration of C into carbonates at geological timescale. However, the carbonate subcycle mentioned above only involves CO_2 as a proton donor. If other acids (such as sulfuric, nitric or organic acids) provide the required acidity, carbonate weathering may lead to CO_2 production instead of CO_2 sequestration, at least transiently (Lerman and Wu, 2006; Calmels et al., 2007). Sulfuric acid is one of these acids that can be produced naturally by oxidation of sulfides and

* Corresponding author. Tel.: +86 851 5891954; fax: +86 851 5891609.
E-mail address: hanguilin@vip.skleg.cn (G. Han).

0012-821X/$ – see front matter © 2008 Elsevier B.V. All rights reserved.
doi:10.1016/j.epsl.2008.02.039

anthropogenically by coal combustion. In parallel to Eq. (1), the carbonate subcycle involving sulfuric acid is:

$$2CaCO_3 + H_2SO_4 \rightarrow 2Ca^{2+} + 2HCO_3^- + SO_4^{2-} \rightarrow CaCO_3 + CO_2 + SO_4^{2-} + Ca^{2+} \quad (2)$$

In this case, carbonate weathering may become a source of CO_2 to the atmosphere/ocean system. Thereafter, on a ten million year timescale, the reduction of sulfate ion associated with organic matter mineralization in sediment pore fluids produces sulfide minerals and alkalinity that reacts with oceanic calcium to balance the CO_2 budget. However, due to the longer residence time of sulfate compared to that of carbonate ions in the ocean, transient effects of CO_2 degassing can be expected as a result of the chemical weathering of carbonate rocks by sulfuric acid. This release of CO_2 might counterbalance part of the CO_2 sequestrated by silicate weathering and has potential climatic implications.

Sulfuric acid as a weathering agent has been recognized recently (Hercod et al., 1998; Galy and France-Lanord, 1999; Anderson et al., 2000; Karim and Veizer, 2000; Yoshimura et al., 2001; Spence and Telmer, 2005; Calmels et al., 2007). However, the importance of chemical weathering of minerals by sulfuric acid is poorly explored. This may be partly due to the difficulty in distinguishing riverine SO_4^{2-} derived from sulfide oxidation from that derived from sedimentary gypsum dissolution. This difficulty is resolved by using combined sulfur and oxygen isotopes (Karim and Veizer, 2000; Pawellek et al., 2002; Calmels et al., 2007).

In this study, we show that elemental ratios and C isotopic ratios of DIC in spring and river water from Guizhou Province, Southwest China can be used to evaluate the importance of sulfuric acid in carbonate weathering and we consider its short- and long-term environmental consequences.

2. Geographical setting of drainage catchments

Guizhou Province is located in the center of the Southeast Asian Karst Region, which is the largest karst area in the world, spreading 17.6×10^4 km^2 with a mean runoff of 400 mm/yr. Guizhou Province is covered dominantly by organic- and sulfide-rich limestone. Coal-bearing rich formations are also widely distributed.

The study area is located between 25° and 27°N latitude and 104° to 106°E longitude (Fig. 1). The region is drained by Beipanjiang River, one of the largest tributaries of Xijiang River (Pearl River). Upstream basins were chosen as a target here because carbonate rocks strata are widely distributed. Landscape of the Guizhou plateau is a typical and spectacular karst landform developed on the Permian and Triassic carbonate rocks (Han and Jin, 1996).

A seasonal monsoonal climate results in high precipitation during summer but much less during winter. Mean annual precipitation in the studied area, averaged over several years, varies from 1000 to 1500 mm. Precipitation decreases from south to north and from east to west. The dominant vegetation in this area is grasslands (above 1000 m) and degraded dry forest and crops (rice, vegetables) evolved from previous natural subtropical forest due to intense agricultural practices. Anthropogenic pressure is considerable as about 30 million people live in Guizhou Province. The land clearance and deforestation have significantly enhanced soil erosion. Because coal is the major energetic resource, the region has been characterized by high rate of acid deposition for a couple of decades (Lei et al., 1997; Han and Liu, 2006). Emissions of SO_2 associated with coal combustion have considerably increased in China since the 1970s, leading to significant deposition of acid rain. In China, the estimated emissions of SO_2 to the atmosphere were about 22 million metric tons in 2003 (Larssen et al., 2006).

3. Samples and analyses

Water samples were collected in July 2005 from both rivers and springs (Fig. 1). Most samples are located in the Beipanjiang River catchment except a couple of samples. Temperature, electrical conductivity and pH of the water samples were measured at the time of sampling. Alkalinity was measured by HCl titration within 12 h after sampling. Major cations (Mg^{2+}, Ca^{2+}, K^+, and Na^+) and anions (SO_4^{2-}, Cl^-, and NO_3^-) were analyzed on 0.2 μm filtered samples. Samples for cation analysis were acidified to pH 2 with ultrapurified HNO_3^-. Major ions were firstly determined by Ionic Chromatography Dionex 120 (with an error of 5%) at IPGP (Institut de Physique du Globe de Paris, France) and then repeated at the State Key Laboratory of Environmental Geochemistry (Guiyang, China) using Dionex ICS 90 for anions (with an error of 5%) and Inductively Coupled Plasma-Optical Emission Spectrometry for cations (with an error of 3%). The difference of ion concentration between the two laboratories is within the error. SiO_2 concentrations were measured by spectrophotometry (molybdenum complex) at the State Key Laboratory of Environmental Geochemistry in Guiyang.

For the determination of concentration and $\delta^{13}C$ of DIC, samples were collected in polyethylene bottles with air-tight caps and preserved with $HgCl_2$ to prevent biological activity. Waters were filtered by pressure filtration through 0.45 μm cellulose-acetate filter paper. Using a modified method of (Atekwana and Krishnamurthy, 1998), 10 ml water sample was injected by syringe into glass bottles that were pre-filled with 1 ml 85% phosphoric acid and magnetic stir bars. The CO_2 was extracted and purified after cryogenic removal of H_2O using a liquid nitrogen–ethanol trap. Finally, the CO_2 was transferred cryogenically into a tube for isotope measurement. For $\delta^{13}C$ analysis of particulate organic carbon (POC), 200 ml to 2000 ml water was filtered through a pre-combusted Whatman GF/F filter (47 mm Ø). The particulate inorganic carbon on the filter was removed by adding 1 N HCl. The POC was then transferred into a tube and combusted at 850 °C with CuO and Cu (Tao et al., 2001) to convert it into CO_2.

Carbon isotopic ratios of DIC and POC were determined on Finnigan MAT 252 mass spectrometer at the State Key Laboratory of Environmental Geochemistry and reported in the notation relative to PDB in per mil, as follows

$$\delta^{13}C = \left[\frac{(^{13}C/^{12}C)_{sample}}{(^{13}C/^{12}C)_{standard}} - 1\right] \times 1000 \quad (3)$$

The $\delta^{13}C$ measurement has an overall precision of 0.1‰. A number of duplicate samples were measured and the results show that the differences were less than the range of measurement accuracy.

4. Results

4.1. Chemical composition of water

The major parameters and ion concentrations of samples are listed in Table 1. The pH values of river water range from 7.4 to 8.7 with mean value of 8.4, which is higher than the mean value (7.8) of spring water. Total dissolved solutes (TDS) of river water and spring water samples vary from 125 to 503 mg/L, with a mean value of 297 mg/L for river water and a slightly higher mean value of 324 mg/L for spring water.

Similar to the Wujiang River (Han and Liu, 2004), Mg^{2+} and Ca^{2+} are the dominant cations while HCO_3^- and SO_4^{2-} are the dominant anions. The $2\times[SO_4^{2-}]+[HCO_3^-]$ over $2\times([Ca^{2+}]+[Mg^{2+}])$ molar ratio gives constant value of 0.93. Ca concentrations range between 637 and 2600 μmol/L with a mean value (close to median value) of 1600 μmol/L. The $[Ca^{2+}]/[Mg^{2+}]$ molar ratio is more variable ranging between 1 and 20 and exhibits a median value of 3.6. This indicates that the Beipanjiang River as well as its tributaries are Mg-rich, reflecting the magnesium-rich nature of Guizhou carbonate and, in a much lesser instance, the possible input of Mg from silicate dissolution. Some spring water samples have high $[Ca^{2+}]/[Mg^{2+}]$ molar ratios, higher than 8, but this value is low compared to the typical $[Ca^{2+}]/[Mg^{2+}]$ of 30 observed in waters draining limestone in the karstic area of the Jura

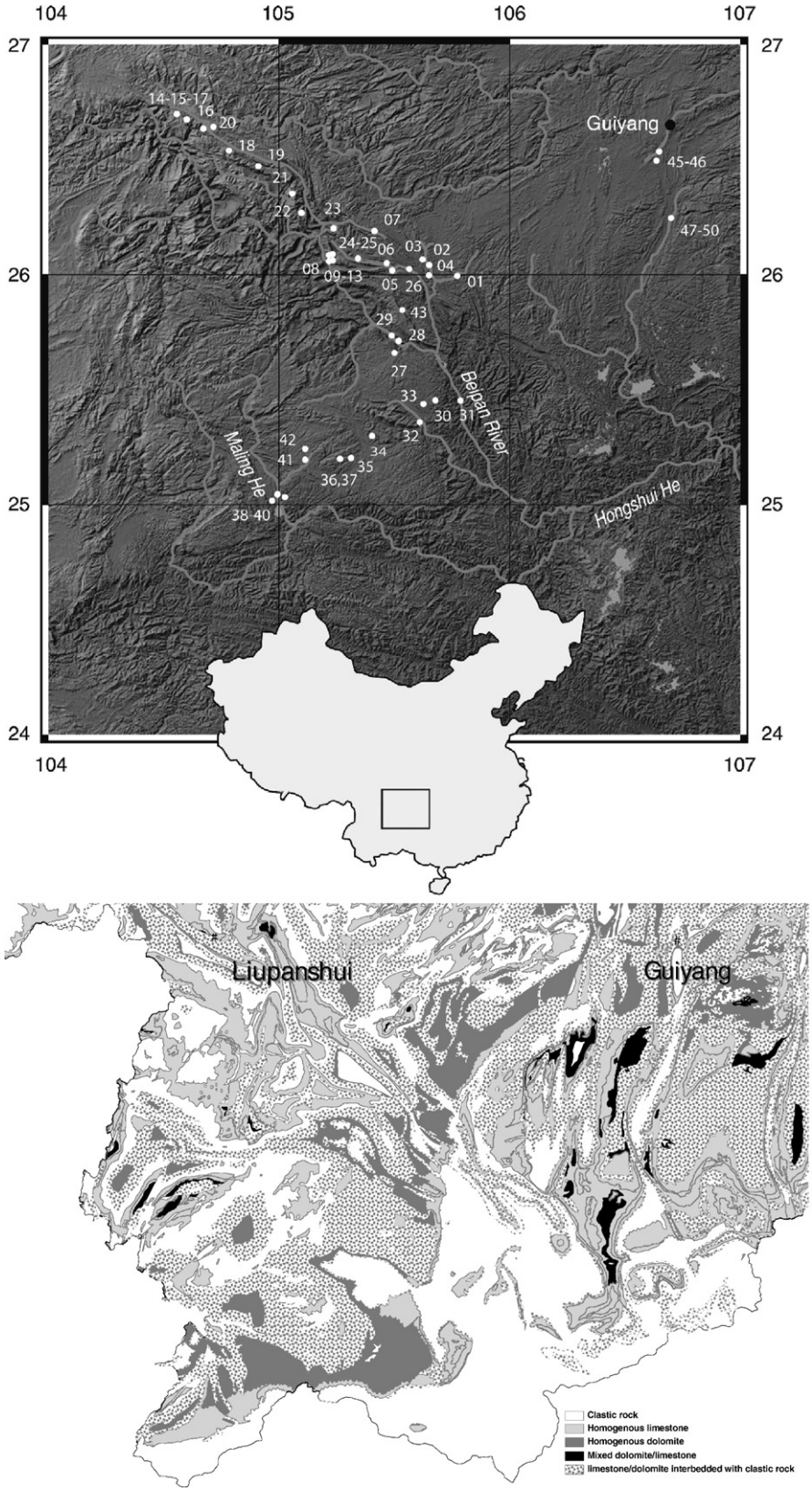

Fig. 1. Topographic and geologic map of the study area.

Mountain in France (Calmels, 2007). Concentration of HCO_3^- ranges from 1000 to 3000 μmol/L with a mean value of 2300 μmol/L in river water samples and from 1900 to 5300 μmol/L with a mean value of 3100 μmol/L in spring water samples. The second major anion is SO_4^{2-} in most water samples, and its concentration averages 660 and 380 μmol/L for river and spring water, respectively. The highest sulfate

Table 1
The chemical and isotope compositions of river and spring waters in the Beipan river catchment, Southwest China

Sample	Type	Latitude	Longitude	Altitude	T	pH	EC	HCO_3^-	Cl^-	SO_4^{2-}	NO_3^-	Na^+	K^+	Mg^{2+}	Ca^{2+}	SiO_2	$\delta^{13}C_{DIC}$	$\delta^{13}C_{POC}$	NICB	log pCO_2	SIc
				(m)	(°C)		(μS/cm)	(μmol/L)									(‰)	(‰)			
CH05-01	River	25°58.205′	105°46.706′	1051	21.1	7.9	363	2564	167	325	148	172	49	299	1456	76	−9.9	−24.6	5	−2.7	0.4
CH05-02	River	25°59.782′	105°40.105′	1032	21.1	8.6	465	2575	125	872	256	321	43	524	1637	58	−10.0	−22.6	0	−3.4	1.1
CH05-03	River	26°01.445′	105°40.398′	1081	20.9	8.5	428	2701	156	567	257	162	48	576	1548	63	−10.1	−24.1	5	−3.3	1.0
CH05-04	River	26°01.404′	105°40.538′	1085	21	8.4	410	2649	144	521	291	149	43	482	1496	56	−8.5	−23.2	1	−3.2	0.9
CH05-05	River	26°02.237′	105°32.026′	1051	19.5	8.0	315	2344	49	320	174	61	27	356	1290	57	−8.9	−24.5	5	−2.9	0.4
CH05-06	Spring	26°02.244′	105°31.842	1061	18.8	7.8	564	2911	69	1197	395	132	35	622	2144	88	−8.7	−27.4	−1	−2.6	0.4
CH05-07	River	26°06 216′	105°25.677′	1209	22.3	7.4	163	1040	33	199	55	122	26	171	627	78	−9.3	−23.9	13	−2.6	−0.8
CH05-08	River	26°02.592′	105°12.623′	595	22	7.6	313	1955	72	389	189	154	28	270	1241	72	−8.7	−21.3	7	−2.5	−0.1
CH05-09	River	26°03.207′	105°13.647′	674	31.8	7.7	689	2585	35	2146	67	226	21	887	2524	89	−2.4	−7.9	1	−2.5	0.5
CH05-10	River	26°04.165′	105°13.964′	754	27.9	8.1	631	2165	12	2060	11	274	20	897	2234	88	−3.7	−12.9	4	−3.0	0.7
CH05-11	River	26°04.972′	105°14.102′	841	25.4	8.4	536	2596	11	1400	49	118	15	617	2132	73	−5.1	−20.8	3	−3.2	1.0
CH05-12	River	26°06.225′	105°14.673′	950	24.6	8.7	371	2344	44	595	50	63	19	303	1535	59	−6.5	−21.4	3	−3.6	1.2
CH05-13	Spring	26°05.837′	105°15.982′	1317	20	7.7	354	2817	35	276	114	18	4	152	1637	55	−11.4	–	2	−2.5	0.2
CH05-14	Spring	26°35.829′	104°44.801′	2131	17.7	7.8	300	2375	12	159	95	22	7	105	1428	65	−11.2	−26.5	10	−2.7	0.2
CH05-15	Spring	26°35.829′	104°44.801′	2147	13	7.7	311	2360	20	231	219	18	9	73	1510	–	–	–	4	−2.6	0.0
CH05-16	River	26°35°910′	104°43.111′	2038	16.6	8.2	305	1976	48	397	164	124	24	338	1201	71	−8.7	−25.6	8	−3.2	0.4
CH05-17	Spring	26°35.754′	104°40.930′	2113	12.9	7.6	291	2431	51	134	274	50	41	387	1109	60	−12.2	−25.5	2	−2.5	−0.2
CH05-18	Spring	26°30.919′	104°58.699′	1731	18.7	7.9	323	2302	62	357	212	42	18	164	1429	48	−9.8	−24.9	−1	−2.8	0.3
CH05-19	River	26°26.735′	105°04.465′	1215	19.8	8.2	374	2197	53	624	191	334	28	321	1376	61	−8.5	−24.4	2	−3.1	0.6
CH05-20	Spring	26°37.806′	104°44.985′	1986	17.7	7.7	305	2512	16	231	58	23	4	173	1448	46	−11.1	−26.5	7	−2.6	0.1
CH05-21	spring	26°19.962′	105°06.563′	1141	21.1	7.9	295	1986	11	408	41	20	9	156	1315	39	−5.2	−25.9	4	−2.8	0.2
CH05-22	spring	26°12.907′	105°07.965′	1105	20.1	8.8	292	1913	53	302	160	32	23	95	1300	50	−8.7	−25.7	4	−3.8	1.1
CH05-23	Spring	26°11.217′	105°14.849′	1142	18.8	8.2	339	2144	43	509	142	45	26	160	1543	46	−9.0	−25.3	4	−3.1	0.6
CH05-24	Spring	26°02.960′	105°30.394′	1154	20.2	8.4	343	2775	32	262	157	23	12	553	1275	46	−10.0	−23.7	5	−3.2	0.8
CH05-25	River	26°02.960′	105°30.394′	1154	22.2	8.3	283	1902	48	301	136	84	27	222	1181	72	−8.7	−24.1	8	−3.3	0.6
CH05-26	Spring	26°01.562′	105°33.969′	1083	20.6	7.7	393	2985	51	328	173	50	34	580	1437	44	−11.4	−22.9	6	−2.5	0.2
CH05-27	Spring	25°34.767′	105°38.101′	1197	23.2	7.7	546	3795	234	408	410	48	6	1208	1575	–	–	–	6	−2.4	0.4
CH05-28	River	25°40.480′	105°39.393′	486	25.3	8.0	332	2081	61	422	171	143	27	297	1367	62	−8.9	−18.8	10	−2.9	0.4
CH05-29	Spring	25°40.358′	105°39.554′	486	22	7.9	598	4898	149	234	406	113	12	293	2651	56	−13.1	−26.3	2	−2.5	0.9
CH05-30	Spring	25°23.406′	105°42.406′	600	22.2	8.1	434	3447	139	326	181	137	33	632	1572	49	−9.6	−24.5	3	−2.8	0.7
CH05-31	River	25°22.719′	105°47.135′	355	22.3	8.0	335	2165	81	445	190	165	32	325	1292	76	−8.7	−22.0	3	−2.9	0.4
CH05-32	River	25°21.336′	105°36.716′	856	24.9	7.9	382	1724	67	902	121	86	36	531	1348	48	−8.7	−24.6	4	−2.9	0.2
CH05-33	Spring	25°21.683′	105°36.777′	894	20.5	7.3	373	2995	31	278	171	21	6	288	1659	27	−11.8	–	4	−2.1	−0.1
CH05-34	Spring	25°14.834′	105°29.139′	1142	20.4	6.9	537	5318	61	142	123	32	11	1254	1616	43	−11.3	–	0	−1.4	−0.3
CH05-35	River	25°07.067′	105°15.410′	1185	22.6	7.9	375	2964	50	285	175	72	25	410	1494	69	−10.3	−23.8	4	−2.6	0.4
CH05-36	Spring	25°07.070′	105°09.282′	1247	19.8	7.1	459	4183	79	182	194	85	21	325	2032	81	−11.2	−26.6	0	−1.7	−0.1
CH05-37	Spring	25°07.878′	105°09.405′	1247	20.1	7.3	562	4309	89	601	230	108	31	855	2119	69	−10.5	−20.8	4	−1.9	0.1
CH05-38	Spring	25°11.641′	104°54.527′	977	21.3	7.4	562	4193	94	645	252	93	44	776	2115	63	−11.2	−25.0	2	−2.0	0.2
CH05-39	Spring	25°11.641′	104°54.527′	977	21.1	8.4	551	–	84	649	244	90	47	764	2077	–	–	–		−3.3	1.0
CH05-40	River	25°11.657′	104°54.664′	971	23.3	8.3	390	2207	86	646	229	157	33	467	1427	65	−9.3	−24.3	4	−3.2	0.7
CH05-41	Spring	25°15.613′	105°03.398′	1395	21.4	7.9	371	2848	50	239	190	43	27	253	1532	46	−11.2	−23.7	2	−2.7	0.4
CH05-42	River	25°15.534′	105°03.388′	1401	20.6	8.7	391	3037	55	232	249	51	35	329	1651	45	−11.1	−23.7	6	−3.5	1.3
CH05-43	Spring	25°26.635′	105°12.990′	1355	21.3	7.5	467	3962	75	232	170	54	35	883	1542	40	−9.4	−27.6	5	−2.2	0.2
CH05-44	River	25°53.488′	105°35.339′	991	23.7	8.4	435	3016	103	480	184	84	40	668	1524	50	−9.8	−24.8	5	−3.2	1.0
CH05-45	River	26°26.261′	106°38.611′	1103	26.9	8.4	430	2585	144	659	224	105	52	559	1500	34	−7.2	–	0	−3.2	1.0
CH05-46	Spring	26°26.497′	106°38.906′	1127	20.4	7.6	579	3510	176	1041	290	181	35	679	2184	49	−10.7	−28.6	−2	−2.3	0.3
CH05-47	River	26°08.382′	106°39.814′	957	26.9	8.5	372	2218	52	604	90	56	24	430	1425	40	−8.1	−25.3	6	−3.4	1.0
CH05-48	Spring	26°08.455′	106°40.150′	983	18.6	7.9	347	2817	44	249	128	35	14	262	1516	51	−11.5	−24.3	3	−2.7	0.4
CH05-49	River	26°08.476′	106°40.019′	979	26.7	8.6	358	2712	79	375	54	80	29	588	1263	44	−9.1	−25.9	6	−3.4	1.1
CH05-50	Spring	26°08.359′	106°40.112′	970	18.3	7.9	349	2838	42	247	129	34	13	260	1509	56	−11.4	–	2	−2.7	0.4

Concentrations are in μmol/L. –: not determined; NICB = $200*(\sum^+ - \sum^-)/(\sum^+ + \sum^-)$ where $\sum^+$ and $\sum^-$ are cationic and anionic charge in μeq/L, respectively.

concentrations (1400 to 2100 μmol/L) are measured in three small streams draining blackshale. In these rivers, the $[HCO_3^-]/[SO_4^{2-}]$ molar ratio is close to 1. All other samples have higher $[HCO_3^-]/[SO_4^{2-}]$ molar ratios ranging from 3 to 37.

Concentrations of Cl^-, NO_3^-, K^+, Na^+ and SiO_2 are relatively low. The Cl^- concentrations range from 11 μmol/L to 234 μmol/L (mean value of 70 μmol/L), about 7 times higher than the mean Cl^- concentrations observed in the rainwater near Guiyang city (Han and Liu, 2006). This high Cl^- concentration cannot be explained by local evapotranspiration and thus shows that anthropogenic activities (over than those integrated in rainwater) are impacting the surface waters sampled here. Na^+ concentrations partly follow those of Cl^-. On a diagram showing Cl^- versus Na^+ normalized concentrations (Fig. 2), most of the spring samples define a straight line, characterized by $[Na^+]/[Cl^-]$ of 1. This trend probably represents an anthropogenic effect (municipal activities, agriculture) because no halite deposits are known in the area. In Fig. 2, most river samples deviate from the 1:1 line showing a Na^+ excess such as the rivers draining blackshales (samples CH05-9, CH05-10, CH05-11). This excess of Na^+ is most likely due to the chemical weathering of silicates. A couple of rivers, however, fit the 1:1 line, indicating that those waters are of karstic-type and not significantly impacted by silicate weathering (samples CH05-1, 3, 4, 44, 45, 49 and 50). Most of the river samples have $[Na^+]/([Ca^{2+}]+[Mg^{2+}])$ molar ratios close to 0.1, while the karstic-dominated waters typically have lower values (0.01–0.05). Note that the rainwater of Guizhou Province, collected near Guiyang, (Han and Liu, 2006) shows a strong enrichment in Cl^- relative to Na^+, possibly explaining the deviation of some data points toward $[Cl^-]>[Na^+]$ values.

As Na^+ and Cl^-, NO_3^- content is indicative of a strong anthropogenic impact on surface water. NO_3^- concentrations range from 10 to 400 μmol/L (mean value of 177 μmol/L). These numbers are not consistent with the NO_3^- concentrations observed in the rain (median value of 21 μmol/L), showing that NO_3^- is mostly of agricultural origin. NO_3^- and Cl^- only show crude correlation, which is probably due to the non-conservative behavior of NO_3^-. Finally, the karstic waters of the Guizhou Province show relatively high SiO_2 concentrations, ranging

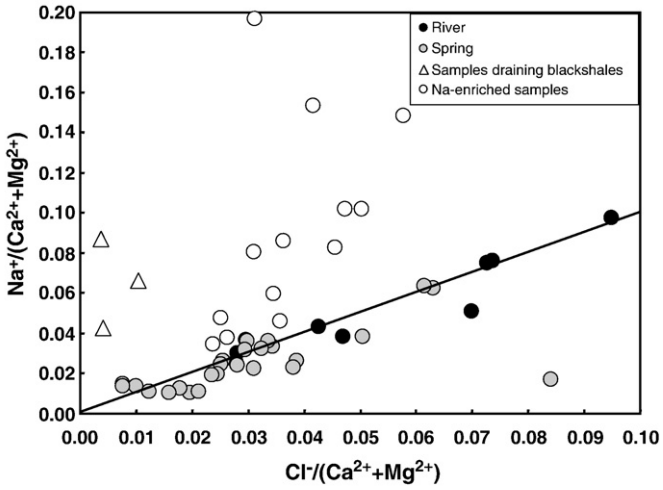

Fig. 2. Cl/Ca+Mg vs. Na/Ca+Mg diagram. Samples lying on the 1:1 line or slightly below are contaminated by anthropogenic sources. They correspond to river and spring water samples. Samples showing enrichment in Na are impacted by silicate weathering. Na-enriched samples are essentially river samples. Small streams draining blackshales have been represented separately. They show low anthropogenic load, but strong silicate contribution.

between 30 and 90 µmol/L. The $[SiO_2]/([Ca^{2+}]+[Mg^{2+}])$ molar ratios only exhibit a slight difference between the water samples dominated by carbonate dissolution (0.01 to 0.025) and those partly influenced by silicate weathering (0.015 to 0.030). A trend of decreasing SiO_2 concentration is observed with increasing $([Ca^{2+}]+[Mg^{2+}])/[Na^+]$. The karstic-dominated waters with $([Ca^{2+}]+[Mg^{2+}])/[Na^+]$ molar ratios above 40) have SiO_2 concentrations close to 30–45 µmol/L, only half of the value observed in rivers influenced by silicate weathering. This result shows that Si is not a unique tracer of silicate weathering reaction and that carbonate-dominated water can have significant concentrations of dissolved Si.

In order to calculate the saturation state index with regards to calcite (SIc) and the partial pressure of CO_2 (pCO_2) that should be in equilibrium with water samples, we used the temperature dependence of thermodynamic constants defined by (Plummer and Busenberg, 1982).

pCO_2 and SIc are listed in Table 1. The pCO_2 ranges from $10^{-3.6}$ to $10^{-2.5}$ with a mean value of $10^{-3.1}$ in river water and from $10^{-3.8}$ to $10^{-1.4}$ with a mean value of $10^{-2.6}$ in spring water. These values are higher than that of the atmosphere ($10^{-3.5}$). This typical feature of spring and river water reflects the fact that most water equilibrates with partial pressure of CO_2 in soil, which is higher than the atmospheric CO_2. River samples have lower calculated pCO_2 than the karstic spring samples which show pCO_2 up to 100 times that of the atmospheric value. Most of the water samples are oversaturated with respect to calcite, except two river water samples and four spring samples. Oversaturation with respect to calcite can reach 10–15 but this is a classic feature of rivers draining carbonate. As a comparison, rivers and springs in the Jura Mountains exhibit oversaturation of 3 to 10 (Calmels, 2007).

4.2. $\delta^{13}C$ of DIC and POC in river and spring water samples

The carbon isotopic compositions of DIC are listed in Table 1. The data show a wide range from −11.1‰ to −2.4‰ with a mean value of −8.3‰ for river water and from −13.1‰ to −5.2‰ with a mean value of −10.5‰ for spring water. The $\delta^{13}C$ values of the mainstream, the Beipanjiang River, are close to the median value (−8.7‰) of that in river samples. Spring waters are clearly enriched in ^{12}C, which suggests a larger involvement of biogenic CO_2, ^{13}C-depleted. The values are similar to those from the Ganga–Brahmaputra River system (Galy and France-Lanord, 1999; Singh et al., 2005), the Ottawa River (Telmer and Veizer, 1999), and the Rhône River (Aucour et al., 1999), lighter than those from the Fraser, Skeena and Nass Rivers (Spence and Telmer, 2005), the Indus River system (Karim and Veizer, 2000) as well as the St. Lawrence River (Yang et al., 1996; Hélie et al., 2002), and usually heavier than most rivers draining Deccan Traps (Das et al., 2005). Note that at the pH condition of our water samples, HCO_3^- is the dominant species of DIC and thus the $\delta^{13}C_{DIC}$ is quite similar to the $\delta^{13}C_{HCO3-}$.

The $\delta^{13}C$ values of POC range from −25.9‰ to −7.9‰ for river water and from −28.6‰ to −20.8‰ for spring water. Most C_3 plants have $\delta^{13}C$ values ranging from −24 to −30‰ with an average of about −27‰. In contrast, C_4 plants have $\delta^{13}C$ values ranging from −10‰ to −16‰ with an average of about −12.5‰ (Vogel, 1993). As shown in Fig. 3, the $\delta^{13}C$ range of POC suggests that they are mainly derived from C_3 plants except samples CH05-09 (−7.9‰) and CH05-10 (−12.9‰), which may be more affected by C_4 plants such as corn frequently cultivated in the region.

5. Discussion

5.1. Theoretical sources of DIC in river and spring water

DIC can originate from several sources and be modified by processes occurring along the water pathways. The chemical weathering of carbonate and silicate minerals is most frequently achieved by the dissolution of biogenic or atmospheric CO_2 in soil waters, which contribute to DIC. Part of the water DIC originates from the weathering of bedrock, but shifted, in both concentration and isotopic composition by secondary processes, such as in situ respiration of natural and anthropogenic organic matter or photosynthesis, equilibration of DIC with atmospheric CO_2 (degassing) and carbonate precipitation (Yang et al., 1996; Aucour et al., 1999; Galy and France-Lanord, 1999; Telmer and Veizer, 1999; Karim and Veizer, 2000; Das et al., 2005). We will discuss these processes in the light of the C isotope data here.

The dominant process of CO_2 generation in soil is the decomposition of organic matter during periods of high biological activity and root respiration (Rasse et al., 2001). As a consequence, pCO_2 in soils is usually higher than that of the atmosphere, isolating the atmospheric CO_2 from the bedrock. If the soil is absent or reduced, atmospheric CO_2 is likely to contribute to chemical weathering. Carbon dioxide then combines with water, when it is available, to form carbonic acid, which is a source of protons. In Southwest China, an additional source of protons is provided by sulfuric acid. Sulfuric acid can be generated by two processes: (1) natural oxidation of disseminated pyrite in the

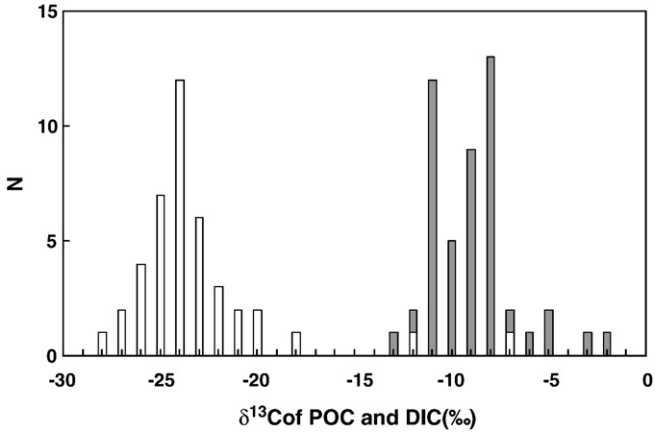

Fig. 3. Histogram comparing the $\delta^{13}C$ values of particulate organic carbon (POC, white bars) and dissolved inorganic carbon (DIC, grey bars) in the rivers and springs of the Guizhou Province. Numbers close to −24‰ are typical of C3 metabolism.

coal-containing strata or (2) reaction between anthropogenic SO_2 from coal combustion in the atmosphere and the free radicals OH and/or aqueous H_2O_2 in droplets (Berner and Berner, 1996). It is recognized that Southwest China is strongly affected by acid rains (Lei et al., 1997). The rainwater data collected in Guiyang City (Han and Liu, 2006) confirm the presence of sulfuric acid in the atmosphere and show common pH values lower than 5.

In summary, the sequence of reactions occurring in soils between bedrock minerals, atmospheric oxygen and water can be described by the following equations:

1. Dissolution of CO_2 from decomposition of organic matter (CH_2O) or from the atmosphere.

$$(CH_2O)_n + nO_2 \rightarrow nH_2O + nCO_2 \quad (4)$$

$$CO_2 + H_2O \rightarrow H_2CO_3 \quad (5)$$

2. Production of sulfuric acid by the oxidative weathering of pyrite or by the oxidation of atmospheric SO_2.

$$FeS_2 + 15/4\ O_2 + 7/2H_2O \rightarrow Fe(OH)_3 + 2SO_4^{2-} + 4H^+ \quad (6)$$

$$SO_2 + 2OH \rightarrow H_2SO_4 \rightarrow SO_4^{2-} + 2H^+ \quad (7)$$

$$SO_2 + H_2O_2 \rightarrow H_2SO_4 \rightarrow SO_4^{2-} + 2H^+ \quad (8)$$

3. Weathering of carbonate minerals by carbonic and sulfuric acids.

$$(Ca_{2-x}Mg_x)(CO_3)_2 + 2H_2CO_3 \rightarrow (2-x)Ca^{2+} + xMg^{2+} + 4HCO_3^- \quad (9)$$

$$(Ca_{2-x}Mg_x)(CO_3)_2 + H_2SO_4 \rightarrow (2-x)Ca^{2+} + xMg^{2+} + 2HCO_3^- + SO_4^{2-} \quad (10)$$

Reaction (10) assumes a complete neutralization of sulfuric acid. In the case of an incomplete neutralization reaction (possible locally, in the vicinity of sulfide minerals or when a solution of low pH dominated by sulfuric acid mixes with a carbonate-saturated water body), the solution is acidic and C is essentially as H_2CO_3. The corresponding equation is:

$$(Ca_{2-x}Mg_x)(CO_3)_2 + 2H_2SO_4 \rightarrow (2-x)Ca^{2+} + xMg^{2+} + 2H_2CO_3 + 2SO_4^{2-} \quad (11)$$

It is interesting to note that, in the rainwater from Guiyang City (Han and Liu, 2006), the samples with the highest pH value show $[SO_4^{2-}]/[Ca^{2+}]+[Mg^{2+}]$ close to 1, indicating that reaction (11) is operating during the incomplete neutralization of sulfuric acid by carbonated dust in the atmosphere.

4. Chemical weathering of silicate minerals.

$$CaSiO_3 + 2H_2CO_3 + H_2O \rightarrow Ca^{2+} + H_4SiO_4 + 2HCO_3^- \quad (12)$$

$$CaSiO_3 + H_2SO_4 + H_2O \rightarrow Ca^{2+} + H_4SiO_4 + SO_4^{2-} \quad (13)$$

where $CaSiO_3$ represents an arbitrary Ca silicate. The nature of silicate minerals disseminated or interbedded with the limestone strata in the Guizhou plateau is not well known. However, Fig. 2 indicates that silicate weathering occurs in the basin and provides part of Na^+, K^+, Mg^{2+} and dissolved Si to surface waters.

5.2. Sources of carbon to the rivers of Guizhou Province

Results from Table 1, particularly the high content of Ca^{2+}, Mg^{2+} and HCO_3^- ions, show that the chemistry of the water in Guizhou Province is dominated by carbonate weathering. This is consistent with the carbonate-dominated nature of the area. Water chemistry also indicates that a significant proportion of Ca and Mg cations are compensated by sulfate anions, suggesting the involvement of sulfuric acid in addition to carbonic acid or gypsum dissolution. In a couple of rivers, silicate weathering is clearly illustrated by the chemistry of water, explaining for example the relatively high Na^+ contents. The sum of $[HCO_3^-]/2*([Ca^{2+}]+[Mg^{2+}])$ and $[SO_4^{2-}]/([Ca^{2+}]+[Mg^{2+}])$ molar ratios is close to 1 in most of the samples, indicating that other cations (Na^+, K^+) and anions (Cl^-, NO_3^-) do not have an important effect on the electric balance in these water samples. The same features have been reported for rivers in Himalaya (Galy and France-Lanord, 1999), the Taroko Gorge area (Yoshimura et al., 2001), the Wujiang River basin (Han and Liu, 2004) and the Western Canadian Cordillera (Gaillardet et al., 2003; Spence and Telmer, 2005) and have been attributed to sulfide oxidation coupled with carbonate weathering.

The $\delta^{13}C$ values of DIC display negative relationship with the $[HCO_3^-]/([Ca^{2+}]+[Mg^{2+}])$ ratio and positive relationships with $[SO_4^{2-}]/([Ca^{2+}]+[Mg^{2+}])$ and $[SO_4^{2-}]/[HCO_3^-]$ ratios (Fig. 4). Assuming that Eqs. (4)–(13) represent the main chemical reactions occurring in soils, we can define the chemical and isotopic signature corresponding to carbonate/silicate weathering by sulfuric/carbonic acids. In a closed system, carbonate weathering reactions lead to water chemistry characterized by $[HCO_3^-]/([Ca^{2+}]+[Mg^{2+}])$ and $[SO_4^{2-}]/([Ca^{2+}]+[Mg^{2+}])$ ratios of 2 and 0 when carbonic acid is involved and 1 and 0.5 when sulfuric acid is involved, respectively (Eqs. (9) and (10)). However, as noted in Eq. (11), degassing of CO_2 can change the above ratios, lowering $[HCO_3^-]/([Ca^{2+}]+[Mg^{2+}])$ (toward 0) and increasing the $[SO_4^{2-}]/([Ca^{2+}]+[Mg^{2+}])$ ratios (toward 1). According to Eq. (12), silicate weathering operated by carbonic acid should lead to $[HCO_3^-]/([Ca^{2+}]+[Mg^{2+}])$ of 2. Actually, Na- and K-silicates are also reacting providing HCO_3^- ions. Based on the elemental ratios from Gaillardet et al. (1999) for waters draining silicates, we suggest that the $[HCO_3^-]/([Ca^{2+}]+[Mg^{2+}])$ ratio of silicate-draining water should be between 3 and 5. Silicate weathering involving sulfuric acid will lead to $[SO_4^{2-}]/([Ca^{2+}])+[Mg^{2+}]$ between 1.5 and 2.5 and $[HCO_3^-]/([Ca^{2+}]+[Mg^{2+}])$ ratios close to 0. The dissolution of sedimentary gypsum would lead to $[SO_4^{2-}]/([Ca^{2+}]+[Mg^{2+}])$ ratios of 1 but there is no geological support for the presence of gypsum in the studied area (see also (Han and Liu, 2004)). In addition, $\delta^{34}S$ of dissolved SO_4^{2-} from Wujiang River shows average values of about −5‰ in summer and −2‰ in winter (Jiang et al., 2005), indicating that most sulfates are derived from the oxidation of sulfide. A gypsum contribution is therefore not considered thereafter.

Carbon isotope ratios in soils are expected to be a result of both source and fractionation effects. Carbon isotopes in marine limestones and dolostones have been extensively reported in the literature and show typical marine values close to 0‰ since the end of the Proterozoic (Telmer and Veizer, 1999). The isotopic composition of CO_2 originated from plant mineralization and root respiration depends on the dominant metabolism pathway. The $\delta^{13}C$ of POC clearly shows that C_3 plants are dominant in the suspended load of the Guizhou water. Indeed, the $\delta^{13}C$ of POC ranges between −20 and −30‰ (mean value −24‰), whereas the mean C isotopic composition of C_3 plants is −26‰. In addition, a slight increase in $\delta^{13}C$ (1 to 4‰) is expected during mineralization of organic matter in the soil (Deines, 1980). The isotopic composition of root-respired CO_2 is expected to be similar to that of plants. Most of the CO_2 produced in the soil diffuses back to the atmosphere and only a small fraction is used for weathering reactions. Diffusion of CO_2 has been shown to cause a slight enrichment in ^{13}C of the gas phase of around 4‰ (Cerling et al., 1991). The extent of the fractionation depends on temperature and CO_2 diffusion rate (Zhang et al., 1995; Clark and Fritz, 1997; Aucour et al., 1999). The C isotopic composition of soil CO_2 reported by previous studies are however close to −24±2‰ (Cerling et al., 1991; Aucour et al., 1999). Prediction of the isotopic composition of DIC under open system conditions (continuous equilibrium with a gas phase of a given pCO_2 and continuous isotopic exchange between CO_2 and the solution) and closed system conditions

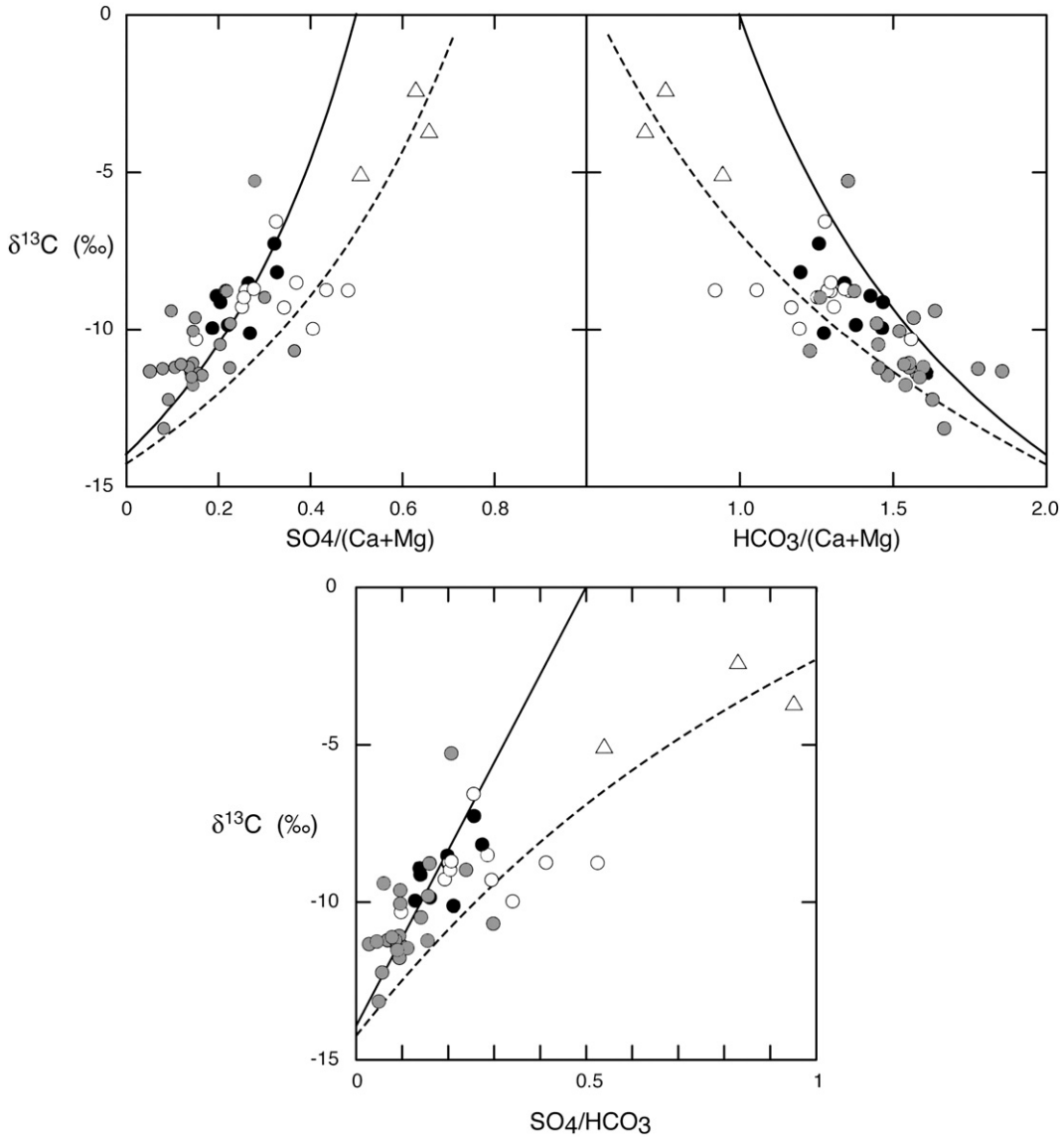

Fig. 4. Diagram showing relationships between carbon isotopes and elemental ratios (in mol/mol) in the river and spring samples. Solid lines correspond to a mixture between the two carbonate weathering endmembers (involving carbonic acid and sulfuric acid, see text for details). Dashed lines are theoretical mixing lines assuming 30% of precipitation after dissolution. Symbols are the same as those in Fig. 2.

(isotopic equilibrium with a gas phase and then isolation from that reservoir before carbonate dissolution) have been made by Deines et al. (1974) and Aucour et al. (1999). With an initial isotopic composition of −24±3‰ for biogenic carbon and 0‰ for carbonates, carbonate weathering by carbonic acid produces DIC with $\delta^{13}C$ values close to −16‰ in open system and −13±2‰ in closed system. Situation is much simpler when sulfuric acid is the proton donor for carbonate weathering as DIC is expected to inherit the isotopic composition of the bedrock.

5.3. Mixing diagrams and mixing proportions

In this section, Fig. 4 is used as mixing diagrams between waters imprinted by carbonate dissolution by carbonic acid and waters influenced by carbonate dissolution by sulfuric acid. All samples without detectable contribution from silicate weathering lie along the theoretical mixing lines in Fig. 4. Contributions from silicate weathering and carbonate weathering are shown in detail in Supplementary data in Appendix A. We will first discuss the case of spring and river water not significantly affected by silicate weathering.

Assuming that degassing of CO_2 does not significantly affect the mixing trends on Fig. 4, the contribution of sulfuric acid as a weathering agent in the karstic province of Guizhou can be modeled by solving the following equations.

$$\left(\frac{HCO_3}{Ca+Mg}\right)_{riv} = \alpha_{sulf}\left(\frac{HCO_3}{Ca+Mg}\right)_{sulf} + \alpha_{carb}\left(\frac{HCO_3}{Ca+Mg}\right)_{carb} \quad (14)$$

$$\left(\frac{SO_4}{Ca+Mg}\right)_{riv} = \alpha_{sulf}\left(\frac{SO_4}{Ca+Mg}\right)_{sulf} + \alpha_{carb}\left(\frac{SO_4}{Ca+Mg}\right)_{carb} \quad (15)$$

$$\delta^{13}C_{riv}\left(\frac{HCO_3}{Ca+Mg}\right)_{riv} = \delta^{13}C_{sulf}\alpha_{sulf}\left(\frac{HCO_3}{Ca+Mg}\right)_{sulf} + \delta^{13}C_{carb}\alpha_{carb}\left(\frac{HCO_3}{Ca+Mg}\right)_{carb} \quad (16)$$

and

$$\alpha_{sulf} + \alpha_{carb} = 1 \quad (17)$$

where the subscripts sulf and carb denote the two endmembers defined by carbonate weathering by sulfuric acid and carbonic acid, respectively. The mixing parameter α_{sulf} denotes the fraction of Ca^{2+}+ Mg^{2+} derived from the sulfuric acid endmember in the water. The best-known parameters are data (within 5% of error) and the unknown ones are the mixing proportions (α), which thus range from 0 to 1. Other parameters, including endmember values, are known with a certain error bar. Given the above discussion, the C isotopic composition of a solution resulting from the interaction of respiratory CO_2 and carbonate is not precisely known and will be affected by a significant error bar. The following values with their errors have been chosen for the two endmembers.

$$([HCO_3^-]/([Ca^{2+}]+[Mg^{2+}]))_{carb} = 2 \pm 0.1$$

$$([SO_4^{2-}]/([Ca^{2+}]+[Mg^{2+}]))_{carb} = 0.00 \pm 0.05$$

$$(\delta^{13}C)_{carb} = -13 \pm 2‰$$

$$([HCO_3^-]/([Ca^{2+}]+[Mg^{2+}]))_{sulf} = 1 \pm 0.1$$

$$([SO_4^{2-}]/([Ca^{2+}]+[Mg^{2+}]))_{sulf} = 0.5 \pm 0.05$$

$$(\delta^{13}C)_{sulf} = 0 \pm 2‰$$

$$\alpha_{sulf} = 0.5 \pm 0.5$$

$$\alpha_{carb} = 0.5 \pm 0.5$$

This set of equations has been solved by an inversion algorithm (Allègre and Lewin, 1989; Negrel et al., 1993; Gaillardet et al., 1999; Roy et al., 1999). This algorithm is used to make all equations and parameters compatible. In this technique, any parameter X of the equations is known with an uncertainty σ and the ratio σ/X reflects our knowledge on the parameter. It can therefore be defined "a priori" values as well as their associated error bar. The main advantage of this procedure is to take into account the "a priori" uncertainty for each parameter. The inversion procedure produces a new set of parameters ("a posteriori" parameters) that best fit all the model equations, generally within an error of about 25%. This algorithm has been applied to all spring and river samples close to the mixing lines on Fig. 4. Results show that the contribution of the sulfuric acid endmember varies from 22% (CH05-36) to 66% (CH05-23 and CH05-21). The mean value is 42±4%, indicating that around 2/5 of the divalent cations in the spring water from Guizhou are originated from the interaction between carbonate minerals and sulfuric acid and that 3/5 of divalent cations are derived from the interaction between carbonic acid and carbonate (Fig. 5). In addition, the inversion procedure allows us to constrain the isotopic composition of the carbonic acid-induced carbonate weathering endmember. The "a posteriori" value of $\delta^{13}C_{carb}$ ranges between −12 and −16‰ (±1) and the mean value for all the spring water samples is −14±1‰, compatible with the discussion of Section 5.2.

As shown in Fig. 4, several data points cannot be explained by the above mixing model. These samples are mainly from rivers and particularly from those where a significant contribution of silicate weathering is detected (Fig. 2) (CH05-9, 10, 11, 6, 2, 32, 46). A first order attempt to correct from silicate weathering is possible using the chemical ratio Ca^{2+}/Na^+, Mg^{2+}/Na^+ and HCO_3^-/Na^+ for silicate derived waters (Gaillardet et al., 1999) and a carbon isotopic composition of the silicate endmember assigned to −25‰. As expected, this correction essentially affects the carbon isotopic composition while chemical ratios only show minor changes. Unlikely values of C isotopic composition up to 4‰ are then calculated indicating that other processes are involved. The presence of gypsum could be a possibility but, it cannot explain the large variability that is observed for C isotopic ratios. In addition, gypsum has not been described in the area by geological surveys. Secondary calcite precipitation may be a possible mechanism shifting $SO_4^{2-}/(Ca^{2+}+Mg^{2+})$ and SO_4^{2-}/HCO_3^- values toward higher values and $HCO_3^-/(Ca^{2+}+Mg^{2+})$ toward lower values. We have shown in Fig. 4 the mixing curves calculated for the case where 30% of Ca^{2+} is removed by carbonate precipitation. Deviation from the mixing lines of some river samples could thus be explained by secondary carbonate precipitation. In addition, these samples usually show higher Mg^{2+}/Ca^{2+} and Sr^{2+}/Ca^{2+} ratios than spring samples that are also consistent with carbonate precipitation. We have thus mainly based our previous and further calculations on spring water samples to prevent from any modification of the geochemical signature of weathering reactions by secondary processes.

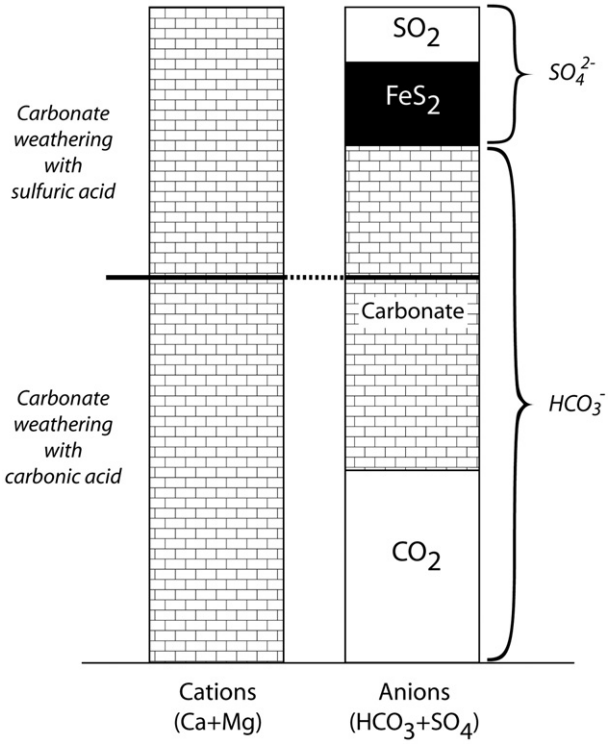

Fig. 5. Histogram of charge balance for an average springwater of the Guizhou Province showing the sources of main cations and anions derived from the calculations of this paper. About 42% of the weathering of Ca and Mg carbonates is due to the action of sulfuric acid and 58% is due to carbonic acid. Sulfate ions are originating from the dissolution of anthropogenic SO_2 in rainwater (40%) and from the oxidative weathering of pyrite disseminated in carbonates or present in the coal-rich strata. About 63% of alkalinity is derived from carbonate rocks.

5.4. Anthropogenic impact on carbonate weathering

Sulfate in water may have several origins. In addition to oxidative weathering of sulfide mineral, acid rain inputs can be significant. Acid rains are a well-known environmental problem in the Southeastern Asia. The low pH of rainwater in China is due to the formation of sulfuric acid derived from the burning of impure coal (Aas et al., 2007; Larssen et al., 2006). As confirmed by rainwater data (Han and Liu, 2006), the study region receives high sulfate concentration from acid rain. The pH values of rainwater in Guiyang range from 3.6 to 6.8 with a mean value of 4.5. The sulfate concentrations range from 30 to 300 µmol/L with a median value of 80 µmol/L (half of the data range from 60 to 110 µmol/L). The $[SO_4^{2-}]/[Cl^-]$ ratio in rain fluctuates widely,

from 1 to 50 with a median value of 8 but half of the data range from 5 to 10. According to these data (see also Supplementary data in Appendix A), the contribution of rainwater sulfate to surface water from Guizhou can be estimated using:

$$[SO_4^{2-}]_{atm} = [Cl^-]_{atm}.(SO_4^{2-}/Cl^-)_{rain} \quad (18)$$

It appears that the amount of SO_4^{2-} derived from the atmosphere varies from a few % in the river water draining the blackshale formations to 90% in some karstic spring waters. The mean contribution of sulfate derived from precipitation represents 40% of the total dissolved SO_4^{2-} in spring water (Fig. 5). Assuming a runoff value of 500–550 mm/yr (Xu and Liu, 2007) corresponding to an evapotranspiration factor of 2 and a median atmospheric SO_4^{2-} input of 160 μmol/L, the Beipanjiang River catchment has a sulfur deposition rate around 3 gS/m^2/yr. This value is consistent with the total sulfur deposition monitored in remote regions in Southwest China by the Integrated Monitoring Program on Acidification of Chinese Terrestrial Systems (IMPACTS, Aas et al., 2007).

The absence of relation between the sulfate concentrations corrected from the rain input and the above used indexes of domestic and agriculture inputs (see also Supplementary data in Appendix A) suggests that the amount of SO_4^{2-} derived from anthropogenic activities other than those integrated by rainwater, is not significant with regard to the total riverine SO_4^{2-} concentration. We therefore attribute all the precipitation-corrected sulfate concentration to sulfide oxidation. If sulfate from sewage and agriculture is significant in some samples, we would over-estimate the importance of bedrock sulfide oxidation.

Based on the mean $([Ca^{2+}]+[Mg^{2+}])/[Cl^-]$ ratio of Guiyang rainwater, we estimated that 2–5% of the divalent cations in spring water are from rainwater. Thus, the chemical weathering of carbonate dust by sulfuric acid in the atmosphere is not significant compared to the weathering rates of bedrocks.

6. Conclusions and consequences for atmospheric CO_2 budget

We demonstrated in this paper that sulfuric acid significantly contributes to the chemical weathering of carbonate rocks in the Guizhou Province, Southwest China. Calculations show that the action of sulfuric acid significantly increases the dissolution of carbonate in this area. In the present paper, on average, 42% of divalent cations are released by the action of sulfuric acid on carbonate rocks in the spring water samples. Two main sources of sulfuric acid are depicted, either from the oxidative weathering of disseminated pyrite or from coal combustion. Our calculations indicate that 40% of the sulfuric acid involved in weathering reactions is of anthropogenic origin. As a consequence, an almost 20% increase of carbonate weathering is observed in the Guizhou Province in response to acid rains. This result is important as it clearly shows that anthropogenic activities can significantly affect rock weathering, even on short timescales. The high dissolution-reactivity of carbonate to anthropogenic sulfuric acid has implications because it not only neutralizes the acidity released to the atmosphere by coal combustion, it also increases the alkalinity of the impacted rivers. The increase of river (and therefore ocean) alkalinity in response to coal combustion can be considered as a positive feedback in the anthropogenic cycle of C and a negative feedback in the acidification of the ocean by the invasion of anthropogenic CO_2. The strength of this negative feedback at a global scale remains to be evaluated but needs more consideration.

This study has implications on the atmospheric CO_2 consumption budget by rock weathering as only 37% of DIC in springs, 1200 μmol/L on average, is derived from the atmosphere whereas 63% have a sedimentary origin, from carbonate (Fig. 5). In cases where chemical weathering reactions of carbonate are only promoted by carbonic acid, these proportions are 50% (see equations, Section 5.1). According to the classical view of the global carbon cycle (Berner and Kothavala, 2001), the chemical weathering of carbonates is not a mechanism that can participate to the amount of CO_2 in the atmosphere because weathering reactions are exactly balanced by the precipitation of carbonate in the ocean. At steady state, the amount of CO_2 annually consumed by carbonate weathering reactions is compensated by an equivalent release of CO_2 in the ocean–atmosphere system during carbonate precipitation. However, as pointed out by Calmels et al. (2007), this subcycle is no longer equilibrated when sulfuric acid is involved as a proton donor in weathering reactions. If sulfuric acid is used, the precipitation of marine carbonate leads to a net release of CO_2 in the ocean–atmosphere system over timescales typical of the residence time of HCO_3^- in the ocean (10^5 yr). At longer timescales, sulfate ions released by sulfuric acid-induced carbonate weathering may be reduced in sediment pore fluids to sulfides, a reaction that produces alkalinity when it is coupled with the oxidation of organic matter. This alkalinity associates with free calcium ions in the ocean to form new carbonate minerals and thus balance the release of sedimentary carbon previously described. As the residence time of SO_4 in the ocean (10^7 yr) is much longer than that of bicarbonate, carbonate weathering by sulfuric acid can lead to the transient release of CO_2 in the ocean–atmosphere system. The weathering of carbonate by sulfuric acid might be thus a transient source of CO_2 to the atmosphere; a statement that contradicts with the conventional view that carbonate weathering is not a significant driver of atmospheric CO_2. It is interesting to note that the transfer of CO_2 from carbonate rocks to the atmosphere can be extremely rapid if secondary carbonate precipitation, from river alkalinity and dissolved Ca+Mg, occurs in lakes or rivers. In this case the release of CO_2 to the atmosphere is much more rapid than when precipitation occurs into the ocean. The extent of carbonate precipitation on lands is not well known and remains to be quantified.

The mean sulfate concentration in spring waters from Guizhou is 390 μmol/L, which is also the amount of CO_2 that will be transiently released to the atmosphere. Using the runoff value of 400 mm/yr (400×10^6 L/km^2/yr) for the region under consideration, we calculate a flux of CO_2 degassing of 1.9 tC/km^2/yr, or 0.33×10^{12} gC/yr for the 17.6×10^4 km^2 of the Guizhou Province. This flux has to be compared with the flux of CO_2 consumed by the weathering of carbonate involving carbonic acid. In the Guizhou Province, the mean concentration of HCO_3^- in springs (3250 μmol/L) leads to a flux of 5.8 tC/km^2/yr and therefore to a flux of 1.0×10^{12} gC/yr consumed from the atmosphere (37% of the total DIC). Extrapolated to the entire surface area of carbonate in Southwest China (54×10^4 km^2), the flux of CO_2 released to the atmosphere–ocean system by sulfuric acid-induced carbonate weathering is 1.0×10^{12} gC/yr while that consumed by carbonic acid-induced carbonate weathering is about 3.1×10^{12} gC/yr. If we only take into account the natural part of sulfuric acid-induced carbonate weathering (without anthropogenic input) the expected flux of sedimentary C from carbonate to the atmosphere in Southwest China is 1.1 tC/km^2/yr or 0.61×10^{12} gC/yr. If the proportions of natural sulfuric vs. carbonic acid found in Southwest China may be generalized (which is, of course, an extreme scenario given the highly reduced nature of carbonates in Southwest China), then a significant global flux of CO_2 degassing is expected to occur (about 29×10^{12} gC/yr) due to the neutralization of sulfuric acid by carbonate rocks. This flux is in the same order of magnitude than that due to volcanism and metamorphism (80×10^{12} gC/yr) and also than the net global flux of atmospheric CO_2 consumed by silicate weathering: 70×10^{12} gC/yr (Gaillardet et al., 1999). However, this generalization implies a larger flux of sulfide oxidation (2.4×10^{12} molS/yr) than that actually assumed at global scale: 0.48×10^{12} molS/yr to 0.65×10^{12} molS/yr (Francois and Walker, 1992; Berner and Berner, 1996; Lerman et al., 2007). As suggested recently (Calmels et al., 2007), the global flux of pyrite oxidation on land might be largely underestimated. This finding is even supported by our study, as, according to the results of this paper, the Southwest

China carbonate area would correspond alone to 8–10% of the conventional global estimate of sulfide oxidation rates. This study therefore opens new perspectives on the processes and the timescales involved in the geological cycle of carbon as well as on the impact of anthropogenic activities on weathering reactions and fluxes.

Acknowledgments

The authors are most grateful to two anonymous reviewers for their helpful insights, which contributed to an obvious improvement of the manuscript. This work was financially supported by the National Natural Science Foundation of China (Grant no. 40673010, 40603005) and Programme de Recherches Avancées de Coopération Franco-Chinoise (Grant no. PRA T04-03) and the IPGP program of CO_2 sequestration (Total, Schlumberger, Ademe). This is IPGP contribution no. 2361.

Appendix A. Estimates of the contributions of carbonate and silicate weathering and corrections of the atmospheric and anthropogenic inputs

The spring and river data of Guizhou Province reported here are strongly impacted by human activities. The contamination of surface water is due to atmospheric contribution, agricultural practices and sewage inputs. Rainwater data have been reported for Guiyang City by Han and Liu (2006). The median value of Cl^-, as shown by the authors to be mostly of anthropogenic origin, is 8 μmol/L. The lowest Cl^- concentrations found in the water in Guizhou Province are between 10 and 20 μmol/L, in good agreement with previous data, assuming an evapotranspiration factor of 2. We therefore consider that these Cl^- values higher than 10–20 μmol/L (median value is 50 μmol/L) are due to other anthropogenic sources than precipitation. The correlation in Fig. 2 shows that most of the karstic spring water samples and some river water samples are characterized by constant $[Cl^-]/[Na^+]$ ratio of 1. A similar trend is observed from the data of Wujiang basin (Han and Liu, 2004) and is attributed to be of anthropogenic origin (agriculture and/or sewage inputs). Cation concentrations can then be corrected from anthropogenic inputs for both rainwater inputs and other anthropogenic inputs using the following equations:

$$[Cl^+]_{atm} = 15 \pm 5\ \mu mol/L$$

$$[Cl^-]_{anthropogenic} = [Cl^-]_{riv} - [Cl^-]_{atm}$$

$$[X]_{atm} = [Cl^-]_{atm} \times ([X]/[Cl^-])_{rainwater}$$

$$[Na^+]_{anthropogenic} = [Cl^-]_{anthropogenic}$$

$[Cl^-]_{anthropogenic}$ and $[Na^+]_{anthropogenic}$ denote the concentrations of Cl^- and Na^+ derived from agriculture and sewage sources. The Na^+ concentration derived from silicate weathering is then calculated by:

$$[Na^+]_{riv} = [Na^+]_{sil} + [Na^+]_{atm} + [Na^+]_{anthropogenic}$$

and the Ca and Mg concentrations are as follows:

$$[Ca^{2+}]_{riv} = [Ca^{2+}]_{sil} + [Ca^{2+}]_{carb} + [Ca^{2+}]_{atm} + [Ca^{2+}]_{anthropogenic}$$

$$[Mg^{2+}]_{riv} = [Mg^{2+}]_{sil} + [Mg^{2+}]_{carb} + [Mg^{2+}]_{atm} + [Mg^{2+}]_{anthropogenic}$$

The median values determined by Han and Liu (2006) for rainwater samples in Guiyang were used ($[Na^+]/[Cl^-]=0.4$, $[Ca^{2+}]+[Mg^{2+}]/[Na^+]=5$). The results of this calculation show that the Na^+ concentration derived from silicate weathering is not significant in all the spring water samples (given the uncertainty on the corrections, we consider that corrected Na^+ concentrations between −30 and +30 μmol/L are not different from zero). Clearly, most of the river samples are influenced by silicate weathering and only a couple of them have no detectable silicate contribution (CH05-01, −03, −04, −05, −44, −45, −47, −49). The highest concentrations of Na^+ derived from silicates (200–300 μmol/L) are observed in the small rivers draining blackshales (CH05-9, CH05-10, CH05-11) and rivers near Huangguoshu waterfall, as well as the Beipanjiang River. Based on a typical HCO_3^-/Na^+ ratio of 3±1 for silicate-draining waters (Gaillardet et al., 1999), we can estimate the amount of DIC derived from silicate weathering in each sample. This contribution is below 5% for all the spring water samples and river water samples with no silicate weathering contribution. It is comprised between a few percent and 40% for the other river samples. This is not surprising because these rivers drain blackshales (CH05-9, 10 and 11), partly redbeds or volcanic rocks (CH05-7, CH05-16). The two Beipanjiang River samples have a contribution of silicate-derived DIC of 15%.

References

Aas, W., Shao, M., Jin, L., Larssen, T., Zhao, D., Xiang, R., Zhang, J., Xiaog, J., Duan, L., 2007. Air concentrations and wet deposition of major inorganic ions at five non-urban sites in China, 2001–2003. Atmos. Environ. 1706–1716.
Allègre, C.J., Lewin, E., 1989. Chemical structure and history of the Earth: evidence from global non-linear inversion of isotopic data in a three-box model. Earth Planet. Sci. Lett. 96, 61–88.
Anderson, S.P., Drever, J.I., Frost, C.K.D., Holden, P., 2000. Chemical weathering in the foreland of a retreating glacier. Geochim. Cosmochem. Acta 64, 1173–1189.
Atekwana, E.A., Krishnamurthy, R.V., 1998. Seasonal variations of dissolved inorganic carbon and $\delta^{13}C$ of surface water: application of a modified gas evolution technique. J. Hydro. 205, 265–278.
Aucour, A.M., Sheppard, S.M.F., Guyomar, O., Wattelet, J., 1999. Use of ^{13}C to trace origin and cycling of inorganic carbon in the Rhône river system. Chem. Geol. 159, 87–105.
Berner, K.E., Berner, R.A., 1996. Global Environment: Water, Air and Geochemical Cycles. Prentice Hall.
Berner, R.A., Caldeira, K., 1997. The need for mass balance and feedback in the geochemical carbon cycle. Geology 25, 955–956.
Berner, R.A., Kothavala, Z., 2001. GEOCARB III: a revised model of atmospheric CO_2 over phanerozoic time. Am. J. Sci. 301, 182–204.
Calmels, D., (2007). Chemical weathering of carbonates: the role of differing weathering agents for global budgets. PhD thesis, University of Paris 7. 248pp.
Calmels, D., Gaillardet, J., Brenot, A., France-Lanord, C., 2007. Sustained sulfide oxidation by physical erosion processes in the Mackenzie River Basin: climatic perspectives. Geology 35, 1003–1006.
Cerling, T.E., Solomon, D.K., Quade, J., Bowman, J.R., 1991. On the isotopic composition of carbon in soil carbon dioxide. Geochim. Cosmochim. Acta 55, 3403–3405.
Clark, I.D., Fritz, P., 1997. Environmental Isotopes in Hydrogeology. LEWIS Publishers.
Das, A., Krishnaswami, S., Bhattacharya, S.K., 2005. Carbon isotope ratio of dissolved inorganic carbon (DIC) in rivers draining the Deccan Traps, India: Sources of DIC and their magnitudes. Earth Planet. Sci. Lett. 236, 419–429.
Deines, P., 1980. The isotopic composition of reduced organic carbon. In: Fritz, P., Fontes, J.C. (Eds.), Handbook of Environmental Isotope Geochemistry. Elsevier, pp. 331–406.
Deines, P., Langmuir, D., Harmon, R.S., 1974. Stable carbon isotope ratios and the existence of a gas phase in the evolution of carbonate ground waters. Geochim. Cosmochim. Acta 38, 1147–1164.
Francois, L.M., Walker, J.C.G., 1992. Modelling the Phanerozoic carbon cycle and climate: constraints from the $^{87}Sr/^{86}Sr$ isotopic ratio of seawater. Am. J. Sci. 292, 81–135.
Gaillardet, J., Dupŕe, B., Louvat, P., Allègre, C.J., 1999. Global silicate weathering and CO_2 consumption rates deduced from the chemistry of large rivers. Chem. Geol. 159, 3–30.
Gaillardet, J., Millot, R., Dupre, B., 2003. Chemical denudation rates of the western Canadian orogenic belt: the Stikine terrane. Chem. Geol. 201 (3–4), 257–279.
Galy, A., France-Lanord, C., 1999. Weathering processes in the Ganges–Brahmaputra basin and the riverine alkalinity budget. Chem. Geol. 159, 31–60.
Han, G.L., Liu, C.-Q., 2004. Water geochemistry controlled by carbonate dissolution: a study of the river waters draining karst-dominated terrain. Chem. Geol. 204, 1–21.
Han, G.L., Liu, C.-Q., 2006. Strontium isotope and major ion chemistry of the rainwaters from Guiyang, Guizhou Province, China. Sci. Total Environ. 364, 165–174.
Han, Z.J., Jin, Z.S., 1996. Hydrology of Guizhou Province, China. Seismology Press.
Hélie, J.-F., Hilaire-Marcel, C., Rondeau, B., 2002. Seasonal changes in the sources and fluxes of dissolved inorganic carbon trough the St. Lawrence River — isotopic and chemical constraint. Chem. Geol. 186, 117–138.
Hercod, D.J., Brady, P.V., Gregory, R.T., 1998. Catchment-scale coupling between pyrite oxidation and calcite weathering. Chem. Geol. 151, 259–276.
Jiang, Y.K., Liu, C.-Q., Tao, F.-X., 2005. Using isotope to trace sulfur cycle, the source and transformation in Wujiang river. Bull. Mineral. Petrol. Geochem. 24 (Suppl.), 325 (in Chinese).
Karim, A., Veizer, J., 2000. Weathering processes in the Indus River Basin: implications from riverine carbon, sulfur, oxygen, and strontium isotopes. Chem. Geol. 170, 153–177.

Larssen, T., Lydensen, E., Tang, D., et al., 2006. Acid rain in China. Environ. Sci. Technol. 15, 418–425.

Lei, H.C., Tanner, P.A., Huang, M.Y., Shen, Z.L., Wu, Y.X., 1997. The acidification process under the cloud in southwest China: observation results and simulation. Atmos. Environ. 31, 851–861.

Lerman, A., Wu, L., 2006. CO_2 and sulfuric acid controls of weathering and river water composition. J. Geochem. Explor. 427–430.

Lerman, A., Wu, L., Mackerzie, F.T., 2007. CO_2 and H_2SO_4 consumption in weathering and material transport to the ocean, and their role in the global carbon balance. Mar. Chem. 106, 326–350.

Negrel, P., Allegre, C.J., Dupre, B., Lewin, E., 1993. Erosion sources determined by inversion of major and trace element ratios in river water: the Congo Basin case. Earth Planet. Sci. Lett. 120, 59–76.

Pawellek, F., Frauenstein, F., Veizer, J., 2002. Hydrochemistry and isotope geochemistry of the upper Danube River. Geochim. Cosmochim. Acta 66, 3839–3854.

Plummer, L.N., Busenberg, E., 1982. The solubilities of calcite, aragonite and vaterite in CO_2–H_2O solutions between 0 and 90 °C, and an evaluation of the aqueous model for the system $CaCO_3$–CO_2–H_2O. Geochim. Cosmochim. Acta 46, 1011–1040.

Rasse, D.P., Francois, L., Aubinet, M., Kowalski, A.S., Vande Walle, I., Laitat, E., Gérard, J.-C., 2001. Modelling short-term CO_2 fluxes and long-term growth in temperate forests with ASPECTS. Ecol. Model. 141, 35–52.

Roy, S., Gaillardet, J., Allegre, C.J., 1999. Geochemistry of dissolved and suspended loads of the Seine river, France: anthropogenic impact, carbonate and silicate weathering. Geochim. Cosmochim. Acta 63, 1277–1292.

Singh, S.K., Sarin, M.M., France-Lanord, C., 2005. Chemical erosion in the eastern Himalaya: major ion composition of the Brahmaputra and $\delta^{13}C$ of dissolved inorganic carbon. Geochim. Cosmochim. Acta 69, 3573–3588.

Spence, J., Telmer, K., 2005. The role of sulfur in chemical weathering and atmospheric CO_2 fluxes: evidence from major ions, $\delta^{13}C_{DIC}$, and $\delta^{34}S_{SO4}$ in rivers of the Canadian Cordillera. Geochim. Cosmochem. Acta 69, 5441–5458.

Tao, F.X., Aucour, A.M., Sheppard, S.M.F., Liu, C.-Q., Leng, X.T., Wang, S.L., Liu, G.S., Xu, W.B., 2001. Evaluation of the sealed-tube low-temperature combustion method for the $^{13}C/^{12}C$ and $^{2}H/^{1}H$ ratio determinations of cellulose nitrate. Chin. J. Chem. 19, 1089–1096.

Telmer, K., Veizer, J., 1999. Carbon fluxes, pCO_2 and substrate weathering in a large northern river basin, Canada: carbon isotope perspectives. Chem. Geol. 159, 61–86.

Vogel, J.C., 1993. Variability of carbon isotope fractionation during photosynthesis. In: Ehleringer, J.R., Hall, E.A., Farquhar, G.D. (Eds.), Stable Isotope and Plant Carbon–Water Relations. Academic Press, pp. 29–38.

Wallmann, K., 2001. Controls on the cretaceous and cenozoic evolution of seawater composition, atmospheric CO_2 and climate. Geochim. Cosmochim. Acta 65 (18), 3005–3025.

Xu, Z., Liu, C.-Q., 2007. Chemical weathering in the upper reaches of Xijiang River draining the Yunnan–Guizhou Plateau, Southwest China. Chem. Geol. 239, 83–95.

Yang, C., Telmer, K., Veizer, J., 1996. Chemical dynamics of the "St. Lawrence" riverine system: δD_{H2O}, $\delta^{18}O_{H2O}$, $\delta^{13}C_{DIC}$, $\delta^{34}S_{sulfate}$, and dissolved $^{87}Sr/^{86}Sr$. Geochim. Cosmochem. Acta 60, 851–866.

Yoshimura, K., Nakao, S., Noto, M., Inokura, Y., Urata, K., Chen, M., Lin, P.-W., 2001. Geochemical and stable isotope studies on natural water in the Taroko Gorge karst area, Taiwan—chemical weathering of carbonate rocks by deep source CO_2 and sulfuric acid. Chem. Geol. 177, 415–430.

Zhang, J., Quay, P.D., Wilbur, D.O., 1995. Carbon isotope fractionation during gas–water exchange and dissolution of CO_2. Geochim. Cosmochim. Acta 59 (1), 107–114.